Investigation of inclusive CP asymmetries in B^0 decays

The ALEPH Collaboration

R. Barate, D. Decamp, P. Ghez, C. Goy, J.-P. Lees, E. Merle, M.-N. Minard, B. Pietrzyk
Laboratoire de Physique des Particules (LAPP), IN²P³-CNRS, 74019 Annecy-le-Vieux Cedex, France

S. Bravo, M.P. Casado, M. Chmeissani, J.M. Crespo, E. Fernandez, M. Fernandez-Bosman, Ll. Garrido[15], E. Graugés, M. Martinez, G. Merino, R. Miquel, Ll.M. Mir, A. Pacheco, H. Ruiz
Institut de Física d'Altes Energies, Universitat Autònoma de Barcelona, 08193 Bellaterra (Barcelona), Spain[7]

A. Colaleo, D. Creanza, M. de Palma, G. Iaselli, G. Maggi, M. Maggi, S. Nuzzo, A. Ranieri, G. Raso[23], F. Ruggieri, G. Selvaggi, L. Silvestris, P. Tempesta, A. Tricomi[3], G. Zito
Dipartimento di Fisica, INFN Sezione di Bari, 70126 Bari, Italy

X. Huang, J. Lin, Q. Ouyang, T. Wang, Y. Xie, R. Xu, S. Xue, J. Zhang, L. Zhang, W. Zhao
Institute of High Energy Physics, Academia Sinica, Beijing, P.R. China[8]

D. Abbaneo, G. Boix[6], O. Buchmüller, M. Cattaneo, F. Cerutti, G. Dissertori, H. Drevermann, R.W. Forty, M. Frank, T.C. Greening, J.B. Hansen, J. Harvey, P. Janot, B. Jost, I. Lehraus, P. Mato, A. Minten, A. Moutoussi, F. Ranjard, L. Rolandi, D. Schlatter, M. Schmitt[20], O. Schneider[2], P. Spagnolo, W. Tejessy, F. Teubert, E. Tournefier, A.E. Wright
European Laboratory for Particle Physics (CERN), 1211 Geneva 23, Switzerland

Z. Ajaltouni, F. Badaud, G. Chazelle, O. Deschamps, A. Falvard, P. Gay, C. Guicheney, P. Henrard, J. Jousset, B. Michel, S. Monteil, J-C. Montret, D. Pallin, P. Perret, F. Podlyski
Laboratoire de Physique Corpusculaire, Université Blaise Pascal, IN²P³-CNRS, Clermont-Ferrand, 63177 Aubière, France

J.D. Hansen, J.R. Hansen, P.H. Hansen[1], B.S. Nilsson, B.Aa. Petersen, A. Wäänänen
Niels Bohr Institute, 2100 Copenhagen, Denmark[9]

G. Daskalakis, A. Kyriakis, C. Markou, E. Simopoulou, A. Vayaki
Nuclear Research Center Demokritos (NRCD), 15310 Attiki, Greece

A. Blondel[12], G. Bonneaud, J.-C. Brient, A. Rougé, M. Rumpf, M. Swynghedauw, M. Verderi, H. Videau
Laboratoire de Physique Nucléaire et des Hautes Energies, Ecole Polytechnique, IN²P³-CNRS, 91128 Palaiseau Cedex, France

E. Focardi, G. Parrini, K. Zachariadou
Dipartimento di Fisica, Università di Firenze, INFN Sezione di Firenze, 50125 Firenze, Italy

A. Antonelli, M. Antonelli, G. Bencivenni, G. Bologna[4], F. Bossi, P. Campana, G. Capon, V. Chiarella, P. Laurelli, G. Mannocchi[5], F. Murtas, G.P. Murtas, L. Passalacqua, M. Pepe-Altarelli
Laboratori Nazionali dell'INFN (LNF-INFN), 00044 Frascati, Italy

A.W. Halley, J.G. Lynch, P. Negus, V. O'Shea, C. Raine, P. Teixeira-Dias, A.S. Thompson
Department of Physics and Astronomy, University of Glasgow, Glasgow G12 8QQ, UK[10]

R. Cavanaugh, S. Dhamotharan, C. Geweniger[1], P. Hanke, G. Hansper, V. Hepp, E.E. Kluge, A. Putzer, J. Sommer, K. Tittel, S. Werner[19], M. Wunsch[19]
Kirchhoff-Institut fř Physik, Universität Heidelberg, 69120 Heidelberg, Germany[16]

R. Beuselinck, D.M. Binnie, W. Cameron, P.J. Dornan, M. Girone, N. Marinelli, J.K. Sedgbeer, J.C. Thompson[14], E. Thomson[22]
Department of Physics, Imperial College, London SW7 2BZ, UK[10]

V.M. Ghete, P. Girtler, E. Kneringer, D. Kuhn, G. Rudolph
Institut für Experimentalphysik, Universität Innsbruck, 6020 Innsbruck, Austria[18]

C.K. Bowdery, P.G. Buck, A.J. Finch, F. Foster, G. Hughes, R.W.L. Jones, N.A. Robertson
Department of Physics, University of Lancaster, Lancaster LA1 4YB, UK[10]

I. Giehl, K. Jakobs, K. Kleinknecht, G. Quast[1], B. Renk, E. Rohne, H.-G. Sander, H. Wachsmuth, C. Zeitnitz
Institut für Physik, Universität Mainz, 55099 Mainz, Germany[16]

A. Bonissent, J. Carr, P. Coyle, O. Leroy, P. Payre, D. Rousseau, M. Talby
Centre de Physique des Particules, Université de la Méditerranée, IN^{2}P^3-CNRS, 13288 Marseille, France

M. Aleppo, F. Ragusa
Dipartimento di Fisica, Università di Milano e INFN Sezione di Milano, 20133 Milano, Italy

H. Dietl, G. Ganis, A. Heister, K. Hüttmann, G. Lütjens, C. Mannert, W. Männer, H.-G. Moser, S. Schael,
R. Settles[1], H. Stenzel, W. Wiedenmann, G. Wolf
Max-Planck-Institut für Physik, Werner-Heisenberg-Institut, 80805 München, Germany[16]

P. Azzurri, J. Boucrot[1], O. Callot, S. Chen, A. Cordier, M. Davier, L. Duflot, J.-F. Grivaz, Ph. Heusse,
A. Jacholkowska[1], F. Le Diberder, J. Lefrançois, A.-M. Lutz, M.-H. Schune, J.-J. Veillet, I. Videau[1], C. Yuan,
D. Zerwas
Laboratoire de l'Accélérateur Linéaire, Université de Paris-Sud, IN^{2}P^3-CNRS, 91898 Orsay Cedex, France

G. Bagliesi, T. Boccali, G. Calderini, V. Ciulli, L. Foà, A. Giassi, F. Ligabue, A. Messineo, F. Palla[1], G. Rizzo,
G. Sanguinetti, A. Sciabà, G. Sguazzoni, R. Tenchini[1], A. Venturi, P.G. Verdini
Dipartimento di Fisica dell'Università, INFN Sezione di Pisa, e Scuola Normale Superiore, 56010 Pisa, Italy

G.A. Blair, G. Cowan, M.G. Green, T. Medcalf, J.A. Strong, J.H. von Wimmersperg-Toeller
Department of Physics, Royal Holloway & Bedford New College, University of London, Surrey TW20 OEX, UK[10]

R.W. Clifft, T.R. Edgecock, P.R. Norton, I.R. Tomalin
Particle Physics Dept., Rutherford Appleton Laboratory, Chilton, Didcot, Oxon OX11 OQX, UK[10]

B. Bloch-Devaux, P. Colas, S. Emery, W. Kozanecki, E. Lançon, M.-C. Lemaire, E. Locci, P. Perez, J. Rander,
J.-F. Renardy, A. Roussarie, J.-P. Schuller, J. Schwindling, A. Trabelsi[21], B. Vallage
CEA, DAPNIA/Service de Physique des Particules, CE-Saclay, 91191 Gif-sur-Yvette Cedex, France[17]

S.N. Black, J.H. Dann, R.P. Johnson, H.Y. Kim, N. Konstantinidis, A.M. Litke, M.A. McNeil, G. Taylor
Institute for Particle Physics, University of California at Santa Cruz, Santa Cruz, CA 95064, USA[13]

C.N. Booth, S. Cartwright, F. Combley, M. Lehto, L.F. Thompson
Department of Physics, University of Sheffield, Sheffield S3 7RH, UK[10]

K. Affholderbach, A. Böhrer, S. Brandt, C. Grupen[1], A. Misiejuk, G. Prange, U. Sieler
Fachbereich Physik, Universität Siegen, 57068 Siegen, Germany[16]

G. Giannini, B. Gobbo
Dipartimento di Fisica, Università di Trieste e INFN Sezione di Trieste, 34127 Trieste, Italy

J. Rothberg, S. Wasserbaech
Experimental Elementary Particle Physics, University of Washington, Seattle, WA 98195 USA

S.R. Armstrong, K. Cranmer, P. Elmer, D.P.S. Ferguson, Y. Gao, S. González, O.J. Hayes, H. Hu, S. Jin, J. Kile,
P.A. McNamara III, J. Nielsen, W. Orejudos, Y.B. Pan, Y. Saadi, I.J. Scott, J. Walsh, Sau Lan Wu, X. Wu,
G. Zobernig
Department of Physics, University of Wisconsin, Madison, WI 53706, USA[11]

Abstract. A search for CP violating effects in the mixing of neutral B mesons is performed using a sample of 4.1 million hadronic Z decays collected with the ALEPH detector from 1991 to 1995. By studying time-dependent asymmetries in flavour-tagged samples of semileptonic and fully inclusive b-hadron decays, two measurements of the semileptonic asymmetry a_{CP} are extracted. No evidence for CP violation is observed, and the combined value $a_{CP} = -0.013 \pm 0.026$ is obtained.

1 Introduction

Since the discovery of CP violation in the neutral kaon system in 1964 [1], the explanation of its origin has been the subject of intense investigation. In the Standard Model, CP violation arises from a complex phase in the Cabibbo-Kobayashi-Maskawa (CKM) quark mixing matrix [2]. Particularly interesting is the potential for studying CP violation in B-meson decays, where a rich phenomenology is expected.

Present efforts are focusing on decay channels of B^0 mesons into exclusive final states, such as B$^0_d \to$ J/ψ K^0_S, which are predicted to have large asymmetries, with little theoretical uncertainty in relating them to the CKM matrix. Recent studies of this channel performed in CDF [3] and at LEP [4,5] gave first indications for a large CP asymmetry. However, the effective branching ratios are small and precision studies of exclusive channels are beyond the reach of LEP.

A complementary approach is to look for CP violation in inclusive asymmetries. Although these asymmetries are predicted to be small in the Standard Model, they provide an interesting possibility to constrain mixing-induced CP

violation, which could be enhanced by the presence of new physics [6].

In each of the two neutral B meson systems, the mass eigenstates B$_H$ and B$_L$ differ from the flavour eigenstates B^0 and $\bar{\text{B}}^0$, and can be described as [6]

$$\text{B}_{\text{L,H}} = p\text{B}^0 \pm q\bar{\text{B}}^0, \tag{1}$$

where p and q are complex mixing parameters with the normalization $|p|^2 + |q|^2 = 1$. CP violation in the mixing results from the mass eigenstates being different from the CP eigenstates, $|q/p| \neq 1$.

This condition manifests itself in different mixing rates for B$^0 \to \bar{\text{B}}^0$ and $\bar{\text{B}}^0 \to$ B^0 in decays to flavour specific final states, which can be observed through the decay rate asymmetry of B^0 and $\bar{\text{B}}^0$ decaying to the "wrong-sign" final state. This is traditionally investigated using semileptonic decays, through a measurement of the so-called "semileptonic asymmetry" defined as

$$a_{\text{CP}} = \frac{\Gamma(\bar{\text{B}}^0 \to \text{B}^0 \to \ell^+\nu\text{X}) - \Gamma(\text{B}^0 \to \bar{\text{B}}^0 \to \ell^-\bar{\nu}\text{X})}{\Gamma(\bar{\text{B}}^0 \to \text{B}^0 \to \ell^+\nu\text{X}) + \Gamma(\text{B}^0 \to \bar{\text{B}}^0 \to \ell^-\bar{\nu}\text{X})} \tag{2}$$

As the proper time dependence of the rates in the above definition cancels out in the ratio, the asymmetry a_{CP} is time-independent. It is often used to parametrize CP violation in the mixing and is directly related to $|q/p|^2$:

$$a_{\text{CP}} = \frac{|p/q|^2 - |q/p|^2}{|p/q|^2 + |q/p|^2}. \tag{3}$$

The CP asymmetry measured with an inclusive sample of B^0 decays, where the flavour state at decay is not identified, can also provide information on the parameter a_{CP}. While the time-integrated rate difference vanishes due to CPT symmetry, a time-dependent asymmetry persists, which is predicted to be [7]

$$\mathcal{A}(t) = \frac{\Gamma(\text{B}^0 \to \text{anything}) - \Gamma(\bar{\text{B}}^0 \to \text{anything})}{\Gamma(\text{B}^0 \to \text{anything}) + \Gamma(\bar{\text{B}}^0 \to \text{anything})} \tag{4}$$

$$= a_{\text{CP}} \left[\frac{\Delta m}{2\Gamma} \sin(\Delta mt) - \sin^2\left(\frac{\Delta mt}{2}\right) \right]. \tag{5}$$

Here, t is the proper decay time of a neutral B meson that was produced as a B^0 or $\bar{\text{B}}^0$; Δm is the mass difference between the mass eigenstates and Γ the decay width (the width difference between B$_H$ and B$_L$ is neglected).

This paper exploits the above considerations to provide two separate measurements of a_{CP} in the B^0_d–$\bar{\text{B}}^0_d$ system based on two samples of semileptonic and fully inclusive b-hadron decays, respectively. For the B^0_d, a_{CP} is predicted in the Standard Model to be $\mathcal{O}(10^{-2})$ or less [8], at the limit of the statistical sensitivity of the data samples considered in these analyses. Because the rapid B^0_s oscillations are not resolved and a_{CP} is expected to be an order of magnitude smaller for the B^0_s, CP violation in the B^0_s–$\bar{\text{B}}^0_s$ system is neglected here. No asymmetry is expected from charged B mesons and b baryons. Other b-hadron sources therefore only dilute the B^0_d asymmetry without changing the time dependence, and no attempt is made to separate B^0_d from other b-hadron decays.

This paper is organized as follows. After a description of the ALEPH detector and the event selection in Sect. 2, the semileptonic and fully inclusive analyses are described in detail in Sects. 3 and 4, respectively. Section 5 gives the prescription for combining the two correlated measurements. Finally the results are summarized in Sect. 6.

2 ALEPH detector and event selection

The analyses are based on 4.1 million hadronic Z decays gathered by ALEPH from 1991 to 1995. A detailed description of the ALEPH detector and its performance is given elsewhere [9,10]. Charged particles are tracked in a two-layer silicon vertex detector (VDET) with double-sided readout (r-ϕ and z), surrounded by a cylindrical drift chamber and a large time projection chamber (TPC), together measuring up to 33 coordinates along their trajectories. These detectors are immersed in a 1.5 T axial magnetic field, providing a resolution on the transverse momentum relative to the beam axis of $\Delta p_{\rm T}/p_{\rm T} = (6 \times 10^{-4})\, p_t \oplus 0.005$ ($p_{\rm T}$ in GeV/c) and a three-dimensional impact parameter resolution of $25\,\mu{\rm m} + 95\,\mu{\rm m}/p$ (p in GeV/c) for tracks having two VDET hits. The TPC also allows particle identification through the measurement of specific ionization (dE/dx). A finely segmented electromagnetic calorimeter of lead/wire-chamber sandwich construction surrounds the TPC. The iron return yoke of the magnet is instrumented with streamer tubes to form the hadron calorimeter, which is surrounded by two additional double layers of streamer tubes for muon identification.

The Monte Carlo simulation, HVFL, is based on JETSET [11] and is described in detail in [12].

During 1998 the LEP1 data were reprocessed using a refined version of the reconstruction program. The main improvements concern the track reconstruction and the particle identification, the main features of which are described elsewhere [13]. The analyses presented here benefit through improved electron identification, b-tagging performance and vertexing efficiencies.

Hadronic events are selected according to the standard ALEPH selection criteria based on charged tracks [14]. The production-vertex position is reconstructed on an event-by-event basis using the constraint of the average beam spot position [15].

For each event, the thrust axis is calculated and the event is divided into two hemispheres using the plane perpendicular to the thrust axis. Events that are outside the VDET acceptance are discarded by requiring $|\cos\theta_{\rm thrust}| < 0.85$, $\theta_{\rm thrust}$ being the angle of the thrust axis with respect to the beam axis.

Lepton candidates (electrons and muons) are searched for as described in [16]. The electron and muon candidates are required to have a momentum greater than $2\,{\rm GeV}/c$ and $2.5\,{\rm GeV}/c$, respectively. In addition, a cut on the dE/dx is applied to reduce the amount of fake muons coming from misidentified kaons.

3 Semileptonic analysis

This section describes the measurement of the CP-violating parameter $a_{\rm CP}$ based on a sample of semileptonic $B_{\rm d}^0$ decays. Since the fraction of mixed $B_{\rm d}^0$ events varies with proper time, a time-dependent study is performed to maximize the sensitivity, and $a_{\rm CP}$ is extracted by a simultaneous fit to the time distributions of events tagged as $B^0 \to B^0$, $B^0 \to \bar{B}^0$, $\bar{B}^0 \to B^0$ and $\bar{B}^0 \to \bar{B}^0$ transitions.

Events in which a b hadron decays semileptonically are selected by means of high-$p_{\rm T}$ leptons. The proper decay time is determined from the primary vertex, the vertex from which the lepton originates and an estimate of the b-hadron momentum. The flavour states at decay time and production time are then inferred from the charge of the lepton and from the hemisphere charge in the opposite hemisphere, respectively.

The identification of b hadrons is based solely on the hard lepton $p_{\rm T}$ spectrum. Jet clustering is performed using the scaled-invariant-mass algorithm [17] with $y_{\rm cut} = 0.004$ [16], and a cut on the transverse momentum $p_{\rm T} > 1.25\,{\rm GeV}/c$ is applied, where $p_{\rm T}$ is computed with respect to the closest jet with the lepton excluded from the jet. If several tracks pass the lepton requirements, the candidate with the highest transverse momentum is selected. Because the lepton candidate is used in the b-vertex reconstruction, at least one three-dimensional hit in the vertex detector is required. Furthermore, the angle between the jet closest to the lepton, taken to be the b jet, and the thrust axis is required to be less than 35°. A total of 131 195 events is selected by these criteria.

3.1 b-hadron reconstruction

The b-decay vertex is reconstructed as the point of closest approach of the charged lepton candidate to the associated jet direction. By construction this procedure is 100% efficient for finding a vertex while giving poorer proper time resolution than previous ALEPH vertex reconstruction procedures. However, this is of little importance as the characteristic time scale of CP asymmetry is $\mathcal{O}(1/\Delta m_{\rm d})$, much longer than the typical time resolution. The total reconstruction efficiency is independent of the true proper time, and the decay length resolution, determined from Monte Carlo, can be described by a sum of three Gaussian functions with widths of $296\,\mu{\rm m}$, $751\,\mu{\rm m}$ and 2.12 mm for 24%, 43% and 33% of the events, respectively.

The decay length resolution in data is studied using tracks that satisfy all selection criteria, except the electron and muon identification. The simulation is checked by comparing the negative tail of the decay length distribution using these tracks for data and Monte Carlo. The width in data is found to be 2% larger than in the Monte Carlo, and this is compensated for in the analysis.

The b-hadron momentum is composed of contributions from the lepton, the neutrino and further charged and neutral decay products. The neutrino energy is estimated

as the missing energy in the hemisphere taking into account the measured mass in both hemispheres [18]. The reconstruction of the remaining contribution is based on a nucleated jet algorithm. Starting with the lepton track associated to the b-hadron decay, charged and neutral particles in the same hemisphere, with energy greater than 0.5 GeV and ordered by decreasing energy, are added until the invariant mass reaches a given cut value. The optimal cut value is determined from Monte Carlo and is parametrized as a function of the neutrino energy, where typical cut values are in the range of 4–5 GeV/c^2. The momentum resolution depends on the momentum and is on average 8% for 55% of the events and 25% for the rest.

After the decay length and momentum are reconstructed, the proper time can be calculated. The reconstruction errors are taken into account by folding the predicted proper time distributions with a resolution function. The resolution function is parametrized from Monte Carlo as a sum of four Gaussian functions with parameters depending linearly on the true proper time.

3.2 Initial and final state tagging

The determination of a_{CP} in the semileptonic analysis is based on the identification of both the initial and final states of the B$_d^0$ meson.

The final state is tagged by the charge of the lepton. The b $\rightarrow \ell^-$ (including b $\rightarrow \tau \rightarrow \ell^-$) and b $\rightarrow$ c̄ $\rightarrow \ell^-$ decays will have a correct final state tag, while in b $\rightarrow$ c $\rightarrow \ell^+$ the charges of the lepton and the decaying b quark have opposite signs, corresponding to a 100% mistag probability. High p_T kaons misidentified as muons mainly originate from the decay chain b $\rightarrow$ c $\rightarrow$ s, and their charge is very likely to have the same sign as that of the b quark. The overall final state mistag probability for fake leptons is estimated from Monte Carlo to be 26%.

Information on the initial state is obtained from the charge of the hemisphere opposite to the lepton candidate. The hemisphere charge is defined as

$$Q_{\text{hemi}} = \frac{\sum_i q_i \, (p_{L,i})^\kappa}{\sum_i (p_{L,i})^\kappa}, \tag{6}$$

where the sum is over all charged tracks in the hemisphere, q_i is the charge of the track, $p_{L,i}$ the projection of its momentum on the thrust axis and $\kappa = 0.5$.

The sign of the opposite hemisphere charge is used to tag the initial state as a B$_d^0$ or a B̄$_d^0$, while its absolute value is used to calculate an event-by-event discriminating variable defined as [19,20]

$$X(Q_{\text{hemi}}) = \frac{w(Q_{\text{hemi}})}{r(Q_{\text{hemi}}) + w(Q_{\text{hemi}})}, \tag{7}$$

where r (w) is the distribution for correctly (incorrectly) tagged signal events. These distributions are extracted from Monte Carlo. A small value of X indicates that the tag is likely to be correct. The average mistag probability for B$_d^0$ using only the hemisphere charge sign is

$(35.5 \pm 0.5)\%$, while the use of the event-by-event value of the discriminating variable gives an effective mistag probability of $(32.7 \pm 0.5)\%$.

The hemisphere charge distributions for both B$_d^0$ and B̄$_d^0$ display a positive offset due to nuclear interactions, which is subtracted to remove the subsequent fake asymmetry. The offset is taken to be equal to the average hemisphere charge in all b events selected in the data for the fully inclusive analysis, which is determined to be 0.00256 ± 0.00015.

Because the value of the hemisphere charge is also used in the tagging, the distributions (i.e. the mean and width) in data and Monte Carlo must be compared. For this purpose, a high purity sample of identified b and b̄ hemispheres is selected by requiring the lepton p_T to be larger than 1.8 GeV/c. Mixed B$_d^0$ decays are suppressed by demanding the sign of the lepton to be equal to the sign of the total charge in the hemisphere containing the lepton, which is correlated to the charge of the initial b quark. The distribution of hemisphere charge in the opposite hemisphere is then fitted with a Gaussian function in both data and Monte Carlo. A discrepancy in the width σ is parametrized by a scaling factor $S = \sigma_{\text{data}}/\sigma_{\text{MC}}$ and a discrepancy in the mean μ by a shift $\delta = |\mu_{\text{data}}| - |\mu_{\text{MC}}|$. The mean μ is obtained by adding the charge distributions for b and b̄ after having flipped the sign of the b̄ hemisphere charge. By construction, the mean μ and hence δ is independent of the global charge offset. The results of this comparison, $S = 1.007 \pm 0.007$ and $\delta = 0.0023 \pm 0.0015$, are used in estimating the systematic errors.

3.3 Fitting procedure

The CP asymmetry a_{CP} is extracted using an unbinned maximum likelihood fit. The sample consists of the following six sources of lepton candidates:

(1) true leptons from b $\rightarrow \ell^-$ including b $\rightarrow \tau^- \rightarrow \ell^-$;
(2) true leptons from b $\rightarrow$ c $\rightarrow \ell^+$;
(3) true leptons from b $\rightarrow$ c̄ $\rightarrow \ell^-$;
(4) true leptons from b $\rightarrow$ J/$\psi \rightarrow \ell^+\ell^-$;
(5) fake and non-prompt leptons from b-hadron decays;
(6) lepton candidates from non-b decays.

The first five sources are further subdivided into four flavour categories: B$_d^0$, B$_s^0$, B$^\pm$ and b baryons. For Sources 4 and 5, the b charge cannot be determined from the lepton charge and certain decay modes for neutral B mesons can be reached from both flavour states. CP violation in these decay modes is neglected. The estimated fraction of each source is given in Table 1. The values were obtained from Monte Carlo and reweighted to the observed amount of fake leptons.

The true initial and final state charges q_0^p, q_0^f are defined to be -1 for b quarks and $+1$ for b̄ quarks. To first order in a_{CP}, the probability distributions $\mathcal{P}_j(t, q_0^p, q_0^f)$ of the true proper time and the true initial and final state charges can be written as [7]

$$\mathcal{P}_j(t, \pm 1, \pm 1) = \frac{e^{-t/\tau_j}}{4\tau_j} \left[1 + \cos(\Delta m_j t) \right], \tag{8}$$

Table 1. Sample composition as determined from the Monte Carlo simulation

Source	Fraction
b $\rightarrow \ell^-$	0.804
b $\rightarrow$ c $\rightarrow \ell^+$	0.071
b $\rightarrow \bar{\text{c}} \rightarrow \ell^-$	0.011
b $\rightarrow$ J/$\psi \rightarrow \ell^+\ell^-$	0.009
Other b-hadron decays	0.008
Non-b decays	0.097

$$\mathcal{P}_j(t, \pm 1, \mp 1) = \frac{e^{-t/\tau_j}}{4\tau_j} \left[1 - \cos(\Delta m_j t)\right] (1 \mp a_j), \quad (9)$$

where τ_j, Δm_j and a_j are the lifetime, oscillation frequency and asymmetry for b-hadron category j with $\Delta m_j = 0$ for B$^\pm$ and b baryons, while $a_j = a_{\text{CP}}$ for B$_{\text{d}}^0$ and $a_j = 0$ for all other b-hadron categories.

The probability distributions of the reconstructed proper time t_{rec} for all sources except Source 6 are given by folding the true proper time distribution with a resolution function R and summing over all four b-hadron categories:

$$h_i(t_{\text{rec}}, q_0^{\text{p}}, q_0^{\text{f}}) = \sum_{j=1}^{4} \int_0^\infty f_{ij} R_i(t_{\text{rec}}, t) \mathcal{P}_j(t, q_0^{\text{p}}, q_0^{\text{f}}) \, dt, \quad (10)$$

where f_{ij} is the fraction of b-hadron Category j in Source i. The fractions of the different b flavours are taken from Monte Carlo simulation with production ratios and lifetimes reweighted to values given in [21]. The semileptonic branching ratios are assumed to be proportional to the b-hadron lifetimes and have been reweighted accordingly. The fractions are normalized to give $\sum_{j=1}^{4} f_{ij} = 1$ for all i. The fraction of B$_{\text{d}}^0$ in the total sample is estimated to be 36%.

Two different resolution functions are used depending on whether the lepton candidate comes directly from the b or via a subsequent charm decay. Sources 1, 4 and 5 therefore use one resolution function and Sources 2 and 3 use another. For Source 6 the distribution is parametrized directly from Monte Carlo and $h_6(t_{\text{rec}}, -1, -1) = h_6(t_{\text{rec}}, +1, +1)$, while $h_6(t_{\text{rec}}, -1, +1) = h_6(t_{\text{rec}}, +1, -1) = 0$ by definition.

The final state flavour q^{f} is given by the charge of the lepton candidate; the probability distribution is

$$g_i(t_{\text{rec}}, q_0^{\text{p}}, q^{\text{f}}) = \xi_i h_i(t_{\text{rec}}, q_0^{\text{p}}, q^{\text{f}}) + (1 - \xi_i) h_i(t_{\text{rec}}, q_0^{\text{p}}, -q^{\text{f}}), \quad (11)$$

where ξ_i is the probability for a correct final state tag for Source i taken to be $\xi = 1$ for Sources 1 and 3, $\xi = 0$ for Source 2, $\xi = 0.5$ for Source 4 and $\xi = 0.74$ for Source 5. The last value is determined from Monte Carlo (see Sect. 3.2). For lepton candidates from non-b decays (Source 6), ξ is defined to be one and all mistagging is contained in the initial state tagging.

For each source the probability density function of X is parametrized for correctly tagged events, $G_i^+(X)$, and

incorrectly tagged events, $G_i^-(X)$. The parametrizations are taken from Monte Carlo. The probability density for an event is then given by

$$\begin{aligned} f(t_{\text{rec}}, X, q^{\text{p}}, q^{\text{f}}) \\ = \sum_i^{6 \text{ sources}} Y_i(X) \left[(1 - M_i(X)) g_i(t_{\text{rec}}, q^{\text{p}}, q^{\text{f}}) \right. \\ \left. + M_i(X) g_i(t_{\text{rec}}, -q^{\text{p}}, q^{\text{f}}) \right], \quad (12) \end{aligned}$$

where the event-by-event mistag probabilities $M_i(X)$ and source fractions $Y_i(X)$ are computed from $G_i^\pm(X)$, the average initial state mistag probabilities η_i and the average source fractions α_i (Table 1) as [19,20]

$$M_i(X) = \eta_i \frac{G_i^-(X)}{G_i(X)}, \quad Y_i(X) = \alpha_i \frac{G_i(X)}{\sum_j \alpha_j G_j(X)}, \quad (13)$$

where $G_i(X) = (1 - \eta_i) G_i^+(X) + \eta_i G_i^-(X)$. Suppressing constant terms, the total likelihood can be written as

$$\mathcal{L} = \prod_j^{N \text{ events}} f(t_{\text{rec},j}, X_j, q_j^{\text{p}}, q_j^{\text{f}}). \quad (14)$$

3.4 Result and consistency checks

The data are fitted with the b-hadron lifetimes and Δm_{d} fixed to the world averages [21], and $\Delta m_{\text{s}} = 50$ ps^{-1}. The result is:

$$a_{\text{CP}} = -0.037 \pm 0.032 \, (\text{stat.}).$$

The distribution of the final state asymmetry, $(N(\ell^+) - N(\ell^-))/(N(\ell^+) + N(\ell^-))$, is shown in Fig. 1. In this figure, the data are divided into two samples according to whether the events are tagged as mixed (Fig. 1a) or unmixed (Fig.1b). In the case of signal events consisting only of perfectly tagged B$_{\text{d}}^0$ and $\bar{\text{B}}_{\text{d}}^0$ mesons, a constant asymmetry equal to a_{CP} is expected in the mixed sample (see (9)), while no asymmetry is expected in the unmixed sample (see (8)). In the real case, background and mistag both dilute the asymmetry; furthermore a small time dependence is introduced. However, the observed asymmetry is still expected to be larger in the events tagged as mixed than in the events tagged as unmixed. As can be seen from Fig. 1, and confirmed by the result of the unbinned likelihood fit for a_{CP}, no significant deviation from zero is observed in the data.

Several checks of the parametrizations used in the fit are performed. The average b lifetime is fitted ignoring tagging information and assuming all b hadrons to have the same lifetime. Only events with a reconstructed proper time between -1.0 ps and 10.0 ps are used in the fit as the resolution becomes dominated by non-Gaussian tails outside this interval and is therefore poorly described. The result, $1.595 \pm 0.007 \, (\text{stat.})$ ps, is consistent with the world average of 1.564 ± 0.014 ps [21], taking into account that there are also significant systematic uncertainties from resolution functions and sample composition. The proper
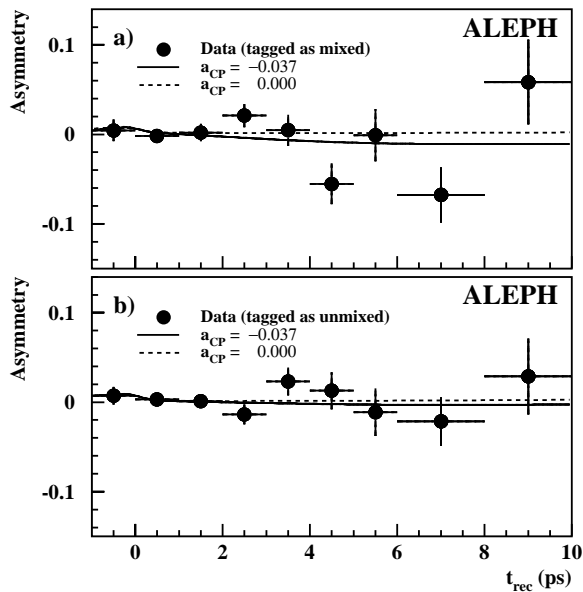
Fig. 1. a Final state asymmetry in events tagged as mixed. **b** Final state asymmetry in events tagged as unmixed. In each plot, the expectation for $a_{\rm CP} = 0$ (dashed line) and the result of the fit for $a_{\rm CP}$ (solid line) have been superimposed. The positive asymmetry at zero proper time is due to fake leptons
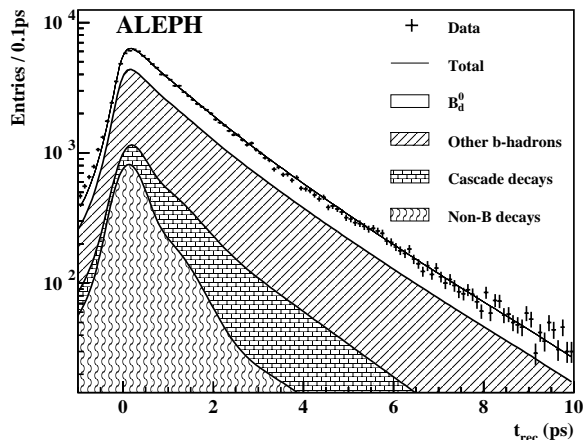

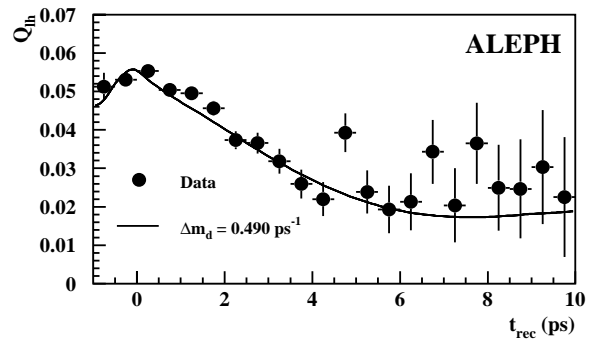**Fig. 2.** Proper time distribution of the selected events and result of the lifetime fit

Fig. 3. Average lepton-signed hemisphere charge $Q_{\ell h}$ as a function of proper time, with the fit result superimposed

Table 2. Results of fits performed using the full sample, only events with proper time larger than 1 ps, only electrons and only muons. Only statistical uncertainties are quoted

Sample	$a_{\rm CP}$
Full	-0.037 ± 0.032
$t > 1$ ps	-0.038 ± 0.032
Electrons	-0.034 ± 0.047
Muons	-0.039 ± 0.044

the average lepton-signed hemisphere charge $Q_{\ell h} = -q_\ell \times Q_{\rm hemi}$ (q_ℓ is the lepton charge) as a function of the reconstructed proper time. This quantity is on average positive for unmixed decays and negative for mixed decays and the figure illustrates the $\rm B_d^0$-$\rm \bar{B}_d^0$ oscillation.

The full fit procedure was tested on a Monte Carlo sample reweighted according to different known values of $a_{\rm CP}$ with no indication for any systematic bias in the fitted value of $a_{\rm CP}$.

As a check, the fit for $a_{\rm CP}$ on data has been repeated with an additional free parameter to allow for a possible asymmetry in the truly unmixed $\rm B_d^0$ events. This asymmetry is found to be consistent with zero, as expected from CPT invariance. Furthermore, a similar check shows no significant asymmetry in the b-hadron background.

3.5 Systematic uncertainties

The systematic uncertainties studied are discussed in the following and listed in Table 3.

b-hadron lifetimes: The b-hadron lifetimes are varied separately within the uncertainties of the world average values.

Sample composition: The fractions of each type of b hadron are varied separately within the uncertainties on the measured values given in [21]. The amount of cascade decays is varied within errors given in [22], while the non-b fraction is varied by 25% as suggested from a comparison between data and Monte Carlo performed in [23]. A relevant background for this analysis comes from charged hadrons misidentified as muons, which give rise to charge

time distribution of signal and background events is shown in Fig. 2. The discrepancy between data and Monte Carlo seen at negative proper times is due to the imperfect description of the resolution mentioned above, but the resolution has little impact on this measurement as the expected CP asymmetry varies slowly with time. The result for $a_{\rm CP}$ does not change significantly when the measurement is restricted to events with proper time larger than 1.0 ps (this removes some of the background) or when fitting electrons and muons separately. The results of these fits are shown in Table 2.

The parameter $\Delta m_{\rm d}$ is fitted using the likelihood expression given above, with $a_{\rm CP}$ set to zero. This yields $\Delta m_{\rm d} = 0.490 \pm 0.022$ (stat.) $\rm ps^{-1}$ consistent with the world average of $0.464 \pm 0.018 \, \rm ps^{-1}$ [21]. Figure 3 shows

Table 3. Summary of systematic uncertainties on a_{CP}

Error sources	a_{CP}
b-hadron lifetimes	0.0016
b-hadron fractions	0.0041
b $\to$ c $\to$ ℓ fraction	0.0013
Δm_s	0.0001
Δm_d	0.0021
Fake leptons	0.0027
Non-b fraction	0.0004
Proper time resolution	0.0002
Hemisphere charge correction	0.0018
Hemisphere charge offset	0.0027
Quadratic sum	0.0066

asymmetries due to secondary interactions with the detector material. The largest effect is observed in the kaon component, which is substantially reduced by the cut in the measured energy loss (Sect. 2). The remaining K$^+$ and K$^-$ contaminations are extracted directly from data using the measured dE/dx distribution of muon candidates. This gives $(1.7 \pm 0.6)\%$ K$^+$ and $(1.1 \pm 0.4)\%$ K$^-$ contamination of the positively and negatively charged muon candidates, respectively. The final state mistag probability for fake leptons is varied by 10% to take into account uncertainties in the hadronic b decays simulated in Monte Carlo.

Δm_s, Δm_d: Δm_s is varied between 9.1 ps^{-1} and 50 ps^{-1}. Because the proper time resolution is not good enough to resolve the rapid B^0_s oscillations, this variation has little effect on the result of the measurement. Δm_d is varied within the uncertainty on the world average value [21].

Resolution: The decay length resolution is varied by 5% in addition to the 2% difference observed between data and Monte Carlo. The resolution due to the momentum measurement is conservatively varied by 10%.

Initial state tagging: For initial state tagging two sources of errors are considered: the hemisphere charge offset and the hemisphere charge distribution itself. The offset is extracted from data and is varied within the statistical uncertainty on the extracted value, 0.00256 ± 0.00015. For the hemisphere charge distribution the width and the mean value are varied separately within the difference given in Table 6 or the uncertainty, whichever is larger.

The final result of the semileptonic analysis is

$$a_{CP} = -0.037 \pm 0.032 \,(\text{stat.}) \pm 0.007 \,(\text{syst.}).$$

4 Fully inclusive analysis

In this analysis, events containing a b hadron are identified by the presence of a secondary decay vertex in combination with a b tag in the opposite hemisphere. An inclusive vertexing technique is used to reconstruct the decay length of the b hadron, and a separate algorithm yields an estimate of the b-hadron momentum. Finally the b flavour at production time is tagged using a multivariate discriminant.

In addition to the event selection described in Sect. 2, the event is required to contain at least two jets defined using the scaled-invariant-mass algorithm with a y_{cut} of 0.01 [15]. The most energetic jet and the jet that forms the highest invariant mass with it are assumed to be the b-hadron jets. In order to suppress three-jet events in which the b-quark pair is not unambiguosly separated into two hemispheres, events with the two selected b-hadron jets in the same hemisphere are rejected.

4.1 Vertexing

In each hemisphere, charged tracks that are likely to come from a secondary vertex are selected based on their pseudorapidity with respect to the jet axis and the impact parameter significance with respect to the primary vertex. These tracks are subjected to a secondary vertex fit. Tracks contributing high χ^2 values are removed from the fit in an iterative procedure. Once a good vertex is found, the procedure is repeated on the remaining tracks. If more than one secondary vertex is found in a given hemisphere, the vertex multiplicity and the reconstructed vertex mass are used to select the best b-vertex candidate. Monte Carlo studies show that only 5% of the tracks assigned to a secondary vertex by this procedure are actually tracks from fragmentation. The resulting average vertexing efficiency is 92% for b hemispheres. The decay length resolution is determined from Monte Carlo and fitted with a sum of three Gaussian functions with widths of $290\,\mu$m, $905\,\mu$m and 3.22 mm for 75%, 22% and 3% of the events, respectively.

The event is required to have a secondary vertex found in at least one hemisphere. If a secondary vertex is reconstructed in both hemispheres, each is used in turn to determine the proper time in the respective hemisphere (denoted as the *same-side* hemisphere in the following) while the other (denoted as the *opposite* hemisphere) is used for b tagging.

4.2 b tagging

Events containing a reconstructed secondary vertex are further enriched in b events by means of a b tag using information from the opposite hemisphere. The b tagging is performed mainly by exploiting the longer lifetime of b hadrons compared to other hadrons, but also by the presence of high-p_T leptons from semileptonic decays and by the mass of secondary vertices. If a secondary vertex is reconstructed successfully in the opposite hemisphere as described in the previous section, then the corresponding decay length d_{vtx} is calculated. For each track in this hemisphere, the track momentum, the pseudorapidity with respect to the jet direction and the χ^2 difference between

assigning the track to the reconstructed secondary vertex and to the primary vertex are combined into a single weight w using a neural network algorithm. These weights quantify the probability for a track to have come from a secondary or the primary vertex, and are used to associate tracks with the secondary vertex and to calculate the resulting vertex mass M_{vtx}. Furthermore, the probability $\mathcal{P}_{hemi}$ of the hemisphere being a b hemisphere based on impact parameters of charged tracks is calculated as described in [15]. Finally the transverse momentum p_T of lepton candidates selected as described in Sect. 2 is used as a discriminating variable, making use of the fact that leptons from semileptonic b decays have a harder p_T spectrum than those from charm decays.

Depending on their availability, up to four variables are then combined into a single discriminant using

$$X_{btag}(x_1, \ldots) = \frac{f_b \prod_i F_i(x_i)}{f_b \prod_i F_i(x_i) + (1 - f_b) \prod_i G_i(x_i)}. \quad (15)$$

Here x_i stands for the variables $\mathcal{P}_{hemi}$, d_{vtx}, M_{vtx} and p_T, f_b denotes the fraction of b events in the sample before applying a b-tag cut and the functions F and G are defined as the probability distributions of the variables x_i for b events and udsc events, respectively.

After an optimized cut on X_{btag}, 1 273 175 hemispheres are selected as b candidates with a purity of 69% and an efficiency of 70%. In addition, X_{btag} is used as a discriminating variable in the maximum likelihood fit described in Sect. 4.5.

4.3 Proper time reconstruction

The momentum of the b hadron is reconstructed using a nucleated jet algorithm similar to that described in Sect. 3.1, with the tracks assigned to the b vertex used as a seed. In order to take into account the missing energy resolution, only a fraction of the missing energy is added. The corresponding correction factor is parametrized as a function of the missing energy and is chosen such as to optimize the momentum resolution. The resulting resolution is a function of the true b-hadron momentum and is 9% on average for 92% of the events.

The b-hadron momentum is combined with the decay length determined from vertexing to calculate the proper time. In order to describe the non-Gaussian tails of the proper time resolution correctly, the shape of the resolution functions used in the fitting procedure are determined from Monte Carlo simulation as a function of true proper time.

4.4 Initial state tagging

The extraction of the CP asymmetry from the reconstructed B^0 candidates requires the determination of their initial flavour state, i.e. whether they were produced as a B^0 or $\bar{B}^0$ state. For this purpose, up to four variables are used, the first three of which are calculated for the opposite hemisphere and one for the same-side hemisphere.

Table 4. Global charge offsets determined from data, with their statistical uncertainties

Variable	Offset
Q_{hemi}	0.00256 ± 0.00015
Q_{vertex}	0.00456 ± 0.00056
Q_{sum}	$0.0345 \ \pm 0.0013$

1. Hemisphere charge: Q_{hemi}, as defined in (6).

2. Vertex charge: $Q_{vertex} = \sum_i w_i q_i$, with weights w_i calculated as described in Sect. 4.2.

3. Signed lepton p_T: If an electron or a muon is identified in the opposite hemisphere, the product of its charge and transverse momentum p_T with respect to the jet axis is calculated after excluding the lepton from the jet. If more than one lepton is found, the candidate with the highest p_T is used.

4. Charge sum: The variable Q_{sum} is defined as the sum of charges of all tracks in the same hemisphere with momentum greater than $0.5 \, GeV/c$, $Q_{sum} = \sum_i q_i$. Since the sum of the charges of tracks originating from the decay of a B^0 or $\bar{B}^0$ is zero, Q_{sum} carries information about the initial flavour only.

Asymmetries in the charge distributions due to secondary interactions with detector material are removed by subtracting offsets from Q_{sum}, Q_{hemi} and Q_{vertex} prior to the tagging procedure. The offsets are directly taken from data, and are listed in Table 4. Another source of charge asymmetries comes from different amounts of positively and negatively charged fake leptons. This effect is however shown to be small compared to the uncertainties mentioned above, and is taken into account in the evaluation of the systematic error.

The four variables defined above are combined into a single discriminant X_{istag} following the prescription used for the b-tagging discriminant. Here the equivalent of f_b in (15) is set to 0.5. The distributions of the discriminating variables and of X_{istag} are displayed in Fig. 4. If events with $X_{istag} > 0.5$ were tagged as B_d^0 and those with $X_{istag} < 0.5$ were tagged as $\bar{B}_d^0$, 31% of the events would be incorrectly tagged on average. The event-by-event value of X_{istag} is used as a discriminating variable in the fitting procedure described in the following section, resulting in an effective mistag probability of 27%.

4.5 Fitting procedure

As described in Sect. 1, the CP violating parameter a_{CP} can be measured from the time-dependent asymmetry $\mathcal{A}(t)$ in tagged samples of B_d^0 and $\bar{B}_d^0$. The time dependence given in (4) assumes however an unbiased inclusive B_d^0 sample, i.e. equal reconstruction efficiencies for all B_d^0 decay modes. In the more general case of differently weighted final states, the asymmetry takes the form [24]

$$\mathcal{A}(t) = c_{CP} \sin(\Delta m_d t) - a_{CP} \sin^2\left(\frac{\Delta m_d t}{2}\right), \quad (16)$$
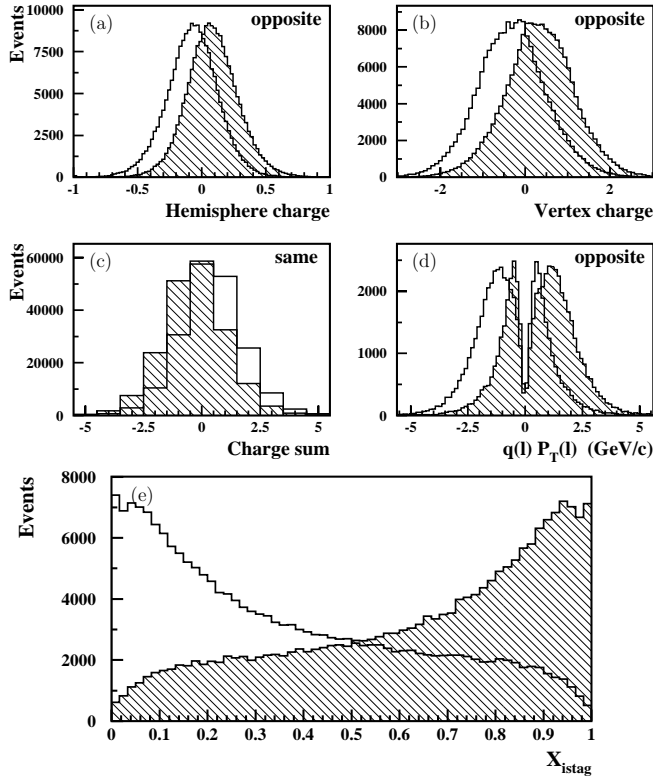
Fig. 4a–e. Distributions of the discriminating variables **a–d** and of the combined discriminant **e** used for initial-state tagging. The open (hatched) histograms are for hemispheres in which a B^0($\bar{\text{B}}^0$) was produced in Monte Carlo

where a_{CP} denotes the semileptonic asymmetry, and c_{CP} is an additional CP violating parameter depending on the relative contributions of different final states. The asymmetry can thus be extracted from a two parameter fit, where the parameter c_{CP} takes into account different selection efficiencies in the various B$_{\text{d}}^0$ decay channels. In case of an unbiased inclusive B$_{\text{d}}^0$ sample, it is predicted to be given by $c_{\text{CP}} = a_{\text{CP}} \Delta m_{\text{d}}/(2\Gamma_{\text{d}})$.

In this analysis, the asymmetry a_{CP} is extracted by means of an unbinned maximum likelihood fit to the proper time distributions of tagged b-hadron candidates. The different contributions to the selected b-hadron sample are grouped into four sources:

(1) mesons produced as B$_{\text{d}}^0$;
(2) mesons produced as $\bar{\text{B}}_{\text{d}}^0$;
(3) other b hadrons;
(4) udsc background.

For the B$_{\text{d}}^0$ and $\bar{\text{B}}_{\text{d}}^0$ signals, the probability distribution of the true proper time t can be written as [7,24]

$$\mathcal{P}_{1,2}(t) = \Gamma_{\text{d}} \exp(-\Gamma_{\text{d}} t)\Big[1 \mp \frac{a_{\text{CP}}}{2}\left(1 - \cos\left(\Delta m_{\text{d}}\, t\right)\right)$$
$$\pm c_{\text{CP}} \sin\left(\Delta m_{\text{d}}\, t\right)\Big], \qquad (17)$$

where $\Gamma_{\text{d}} = 1/\tau_{\text{B}_{\text{d}}^0}$ is the inverse B$_{\text{d}}^0$ lifetime and the upper (lower) sign corresponds to B$_{\text{d}}^0$ ($\bar{\text{B}}_{\text{d}}^0$).

The proper time distribution for other b hadrons is taken to be

$$\mathcal{P}_3(t) = \frac{1}{\tau_{\text{b}}^{\text{eff}}} \exp(-t/\tau_{\text{b}}^{\text{eff}})\,, \qquad (18)$$

where $\tau_{\text{b}}^{\text{eff}}$ denotes the effective lifetime for b hadrons other than B$_{\text{d}}^0$ which is taken from Monte Carlo.

The probability distributions of the reconstructed proper time expected for b events, $h_{1,2}(t_{\text{rec}})$ and $h_3(t_{\text{rec}})$, are obtained by convolving $\mathcal{P}_{1,2}(t)$ and $\mathcal{P}_3(t)$ with the corresponding resolution function and take into account the weak dependence of the selection efficiency $\epsilon(t)$ on true proper time. The efficiencies and resolution functions are parametrized separately for the different b-hadron sources, but independently of the various b decay modes.

The distribution $h_4(t_{\text{rec}})$ of udsc background events, which is determined from Monte Carlo, is directly parametrized as a function of reconstructed proper time.

In order to maximize the sensitivity on the CP violating parameter a_{CP}, the event-by-event values of the discriminating variables for b tagging and initial state tagging are used in the likelihood function. The normalized distributions of X_{btag}, $f_j(X_{\text{btag}})$, are taken to be the same for all b-hadron Sources 1–3, while the distributions of X_{istag}, $g_j(X_{\text{istag}})$, are parametrized separately for each Source j.

The total likelihood function can then be written as

$$\mathcal{L}(a_{\text{CP}}, c_{\text{CP}}) = \prod_i^{N\,\text{events}} \sum_{j=1}^{4} \alpha_j\, f_j(X_{\text{btag},i})$$
$$\times g_j(X_{\text{istag},i})\, h_j(t_{\text{rec},i})\,, \qquad (19)$$

where α_j is the fraction of Source j determined from Monte Carlo, with the production fractions of the individual b-hadron species taken from [21]. The above likelihood expression assumes that the three variables X_{btag}, X_{istag} and t_{rec} are uncorrelated, a condition that is verified in the Monte Carlo at the 1% level. Note that the dependence on the fitted parameters a_{CP} and c_{CP} is contained in $h_{1,2}(t_{\text{rec}})$.

4.6 Results

The fitting procedure is tested on Monte Carlo samples which were reweighted according to different values of a_{CP} and c_{CP}, checking that the fit reproduces the input values. The data are fitted with all physical input parameters fixed to the central values of their world averages [21]. A one-parameter scan of a_{CP} using the likelihood expression described in the previous section, and with the constraint $c_{\text{CP}} = a_{\text{CP}} \Delta m_{\text{d}}/(2\Gamma_{\text{d}})$ gives

$$a_{\text{CP}} = 0.015 \pm 0.033\,(\text{stat.})\,.$$

A second fit, in which both a_{CP} and c_{CP} are allowed to vary independently, yields the result

$$a_{\text{CP}} = 0.016 \pm 0.034\,(\text{stat.})\,,$$
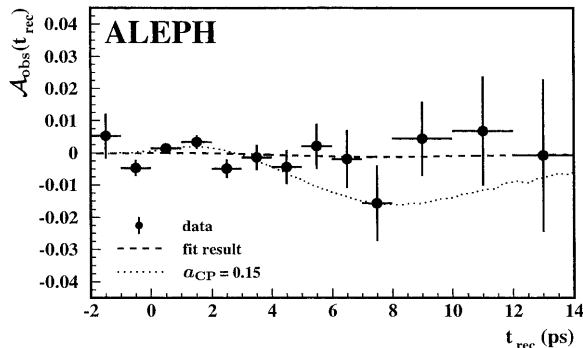$$c_{\text{CP}} = 0.003 \pm 0.017\,(\text{stat.})\,,$$

Fig. 5. Observed time-dependent asymmetry $\mathcal{A}_{\mathrm{obs}}(t_{\mathrm{rec}})$ between tagged $\bar{\mathrm{b}}$ and b hemispheres, with the result of the fit superimposed (dashed line). Also shown for illustration is the predicted curve for $a_{\mathrm{CP}} = 0.15$ (dotted line)

where the correlation of the two parameters is 79%. No significant shift is seen in the fitted value of a_{CP} compared to the one-parameter fit, while the value of c_{CP} is consistent with the assumption of an unbiased inclusive b sample.

The time-dependent asymmetry of tagged $\bar{\mathrm{b}}$ and b hemispheres (4) is shown in Fig. 5, with the result of the measurement superimposed. For the purpose of display, hemispheres with $X_{\mathrm{istag}} > 0.5$ are taken to be $\bar{\mathrm{b}}$ ($\mathrm{B}_{\mathrm{d}}^0$) and those with $X_{\mathrm{istag}} < 0.5$ are taken to be b ($\bar{\mathrm{B}}_{\mathrm{d}}^0$). No obvious time-dependent structure is observed.

4.7 Systematic studies

The following sources of systematic uncertainties are considered.

Physics input parameters: The values of Δm_{d}, $\tau_{\mathrm{B}_{\mathrm{d}}^0}$, and the production fraction of $\mathrm{B}_{\mathrm{d}}^0$ are varied within their world average errors [21] and the uncertainties are propagated to the measured values of a_{CP} and c_{CP}. Similarly the uncertainty arising from $\tau_{\mathrm{b}}^{\mathrm{eff}}$ is obtained by varying each of the contributing b-hadron lifetimes and production fractions by its error.

b tagging: In order to estimate the systematic error due to the b tagging, a fit for the udsc background fraction is performed with all other parameters fixed and ignoring the initial state tagging information. This fit also provides a consistency check of the background parametrization. The fitted value is found to be 0.333 ± 0.001, compared to 0.310 as determined from Monte Carlo. The change of a_{CP} and c_{CP} obtained by varying the background fraction by twice the difference between the fitted and simulated values is taken as a systematic error.

Proper time resolution: The measurement is hardly sensitive to the proper time resolution, as the characteristic time scale of the signal $\mathcal{O}(1/\Delta m_{\mathrm{d}})$ is much larger than the average resolution of approximately 0.2 ps. The sensitivity is estimated by varying the proper time resolution used in the likelihood function by $\pm 5\%$ independently of the true proper time, and by using alternative
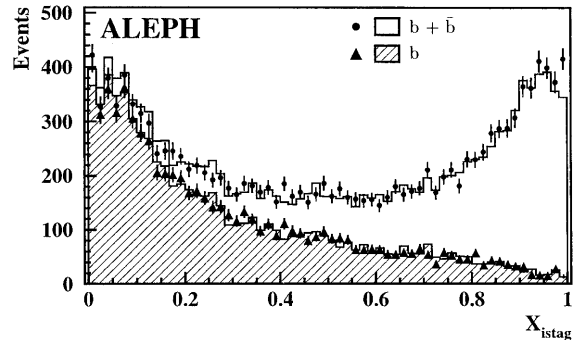

Fig. 6. Distribution of the initial state tagging variable X_{istag} for b and $\bar{\mathrm{b}}$ enriched hemispheres in data (points) and Monte Carlo (histograms)

Table 6. Shifts in the mean values and the scale factors, with their statistical uncertainties, representing the difference between real and simulated charge distributions

Variable	δ	S
Q_{hemi}	$+0.0023 \pm 0.0015$	1.007 ± 0.007
Q_{vertex}	-0.0050 ± 0.0069	1.009 ± 0.006
Q_{sum}	$+0.011 \ \pm 0.011$	1.023 ± 0.006

parametrizations for the resolution functions. None of these variations leads to a change of the measured value of a_{CP} and c_{CP} greater than 10^{-4}.

Initial state tagging: To check the accuracy of the simulation with respect to the tagging discriminant X_{istag}, a comparison between data and Monte Carlo is performed. For this purpose, pure samples of b and $\bar{\mathrm{b}}$ hemispheres are selected as described in Sect. 3.2.

The distributions of X_{istag} in data and Monte Carlo are shown in Fig. 6, with no significant discrepancies. The systematic error on the initial state tagging is assessed by varying the associated discriminating variables according to their estimated uncertainties. The variations are then propagated to the X_{istag} distributions.

The tagging power of Q_{hemi}, Q_{sum} and Q_{vertex} is determined by the charge separation between b and $\bar{\mathrm{b}}$ hemispheres, given by the difference of the mean values μ and the widths σ of the charge distributions. The charge distributions obtained from data and Monte Carlo are compared using the event sample mentioned above. A discrepancy is parametrized in terms of a scaling factor S and a shift δ as defined in Sect. 3.2, except that for Q_{sum} and Q_{vertex} the mean values and the standard deviations of the distributions are used rather than the fitted parameters of a Gaussian function. The charge distributions are then modified according to the observed discrepancies listed in Table 6 or the statistical uncertainty, whichever is larger. Furthermore, the global charge offsets obtained from data are varied within their statistical uncertainties (Table 4).

The power of the signed lepton p_{T} as a discriminating variable is mainly determined by the fraction of cascade decays $\mathrm{b} \to \mathrm{c} \to \ell^+$ compared to direct decays $\mathrm{b} \to \ell^-$.

Table 5. Summary of systematic errors evaluated on $a_{\rm CP}$ and $c_{\rm CP}$

Source	$\Delta a_{\rm CP}$		$\Delta c_{\rm CP}$	
b-hadron lifetimes	+0.0025	−0.0011	+0.0011	−0.0004
b-hadron fractions	+0.0025	−0.0025	+0.0012	−0.0012
$\Delta m_{\rm d}$	+0.0004	−0.0008	+0.0010	−0.0011
Proper-time resolution	< 0.0001	< 0.0001	< 0.0001	< 0.0001
b tagging	+0.0010	−0.0010	+0.0004	−0.0004
Hemisphere/vertex charge offsets	+0.0043	−0.0047	+0.0092	−0.0096
Hemisphere/vertex charge scaling	+0.0070	−0.0053	−0.0025	−0.0019
Fake lepton asymmetry	< 0.0001	< 0.0001	+0.0002	−0.0002
b → c → ℓ fraction	+0.0003	−0.0003	+0.0001	−0.0001
Quadratic sum	+0.0090	−0.0077	+0.0097	−0.0099

This fraction is scaled within its quoted error and the Monte Carlo events that are used to determine the corresponding tagging distributions are reweighted accordingly. Another source of uncertainties is due to misidentified hadrons (fake leptons), which induce a charge asymmetry in the $p_{\rm T}$ distributions. The amount of fake muon candidates (which give the main effect) is varied by the observed difference between data and Monte Carlo, determined as described in Sect. 2.

The systematic errors discussed above are summarized in Table 5. The final results determined from the two-parameter fit are

$$a_{\rm CP} = 0.016 \pm 0.034\,({\rm stat.}) \pm 0.009\,({\rm syst.})\,,$$
$$c_{\rm CP} = 0.003 \pm 0.017\,({\rm stat.}) \pm 0.010\,({\rm syst.})\,.$$

5 Combination of the results

The procedure adopted here to combine the correlated measurements obtained from the semileptonic and fully inclusive analyses follows that of the BLUE (Best Linear Unbiased Estimator) technique [25]. Correlations arise from the fact that the two analyses are based on partially overlapping event samples, as well as from certain systematic uncertainties.

The statistical correlations are estimated using toy Monte Carlo experiments. Events are generated according to the chosen b-hadron and background composition. For each b event, a true proper time is generated using the predicted proper time distributions, including the effects of mixing and CP violation. Effects of the detector resolution are taken into account by smearing the generated values according to the appropriate resolution functions. Initial and final state tags are assigned to each hemisphere, with the tagging-discriminant distributions and correlations between tagging results in both analyses taken from the full Monte Carlo simulation. Finally, selection criteria are applied such that the overlap between both analyses is the same as in the actual data. Each of the toy experiments is then subjected to an unbinned fit using the likelihood expressions described in Sects. 3.3 and

4.5. Using toy experiments, the correlation is found to be $\rho = 0.08 \pm 0.01$ (stat.).

The reliability of the above estimate is checked by varying the relevant input parameters and by changing a variety of model assumptions in the simulation. None of these checks gives a change in the value of ρ greater than ± 0.03.

Common systematic uncertainties that are not explicitly related to a single shared parameter are conservatively treated as fully correlated. Errors are symmetrized prior to the combination procedure, using the largest absolute value of the positive and negative uncertainties.

Combining the two results following the BLUE prescription gives the result

$$a_{\rm CP} = -0.013 \pm 0.026\,,$$

where the quoted error comprises both statistical and systematic uncertainties. The error on the statistical correlation determined as described above is included in the final uncertainties quoted for $a_{\rm CP}$.

As a check, the combination is repeated assuming fully correlated or uncorrelated systematic uncertainties. This leads to a shift in $a_{\rm CP}$ of ± 0.0003 and to a change in the total error of ± 0.0004, demonstrating that the result of the combination is very robust with respect to model assumptions and to the detailed treatment of correlated systematic uncertainties.

6 Conclusions

Using 4.1 million hadronic Z decays collected with the ALEPH detector at LEP, a search for mixing-induced CP violation in the B$_{\rm d}^0$–B̄$_{\rm d}^0$ system has been performed. Two measurements of the CP observable $a_{\rm CP}$ have been extracted from data by investigating time-dependent asymmetries in semileptonic and fully inclusive B$_{\rm d}^0$ decays. No significant asymmetry is observed, and the following results for $a_{\rm CP}$ are obtained:

$$a_{\rm CP} = -0.037 \pm 0.032 \pm 0.007 \quad ({\rm semileptonic\ analysis})\,,$$
$$a_{\rm CP} = +0.016 \pm 0.034 \pm 0.009 \quad ({\rm fully\ inclusive\ analysis})\,.$$

The two measurements are averaged to yield

$$a_{\mathrm{CP}} = -0.013 \pm 0.026 \, ,$$

where the statistical and systematic uncertainties are combined.

This value can be translated into a measurement of the CP violating parameter $\mathrm{Re}\,\epsilon_{\mathrm{B}}$, where $\epsilon_{\mathrm{B}} = (p-q)/(p+q)$ is another commonly used parameter to describe CP violation in the mixing. Using the relation

$$a_{\mathrm{CP}} \approx \frac{4\,\mathrm{Re}\,\epsilon_{\mathrm{B}}}{1 + |\epsilon_{\mathrm{B}}|^2} \tag{20}$$

one obtains

$$\frac{\mathrm{Re}\,\epsilon_{\mathrm{B}}}{1 + |\epsilon_{\mathrm{B}}|^2} = -0.003 \pm 0.007 \, .$$

These results are consistent with measurements from OPAL [26,27], CLEO [28] and CDF [29].

References

1. J.H. Christenson, J.W. Cronin, V.L. Fitch, R. Turlay, "Evidence for the 2π decay of the K_2^0 meson", Phys. Rev. Lett. **13** (1964) 138

2. N. Cabibbo, "Unitary symmetry and leptonic decays", Phys. Rev. Lett. **10** (1963) 531; M. Kobayashi, K. Maskawa, "CP-violation in the renormalizable theory of weak interaction", Prog. Theor. Phys. **49** (1973) 652

3. CDF Collaboration, "Measurement of $sin(2\beta)$ from $B \to J/\psi K_S^0$ with the CDF detector", Phys. Rev. **D 61** (2000) 072005

4. ALEPH Collaboration, "Study of the CP asymmetry of $B^0 \to J/\psi K_S^0$ decays in ALEPH", ALEPH 2000-067 CONF 2000-045, contributed paper #179 to the XXXth International Conference on High Energy Physics, 27 July – 2 August 2000, Osaka, Japan

5. OPAL Collaboration, "Investigation of CP violation in $B^0 \to J/\psi K_S^0$ decays at LEP", Eur. Phys. J. **C 5** (1998) 370

6. See for example A.I. Sanda, Zhi-Zhong Xing, "Search for new physics in CP-violating B decays", Phys. Rev. **D 56** (1997) 6866; L. Randall, Shufang Su, "CP violating lepton asymmetries from B decays and their implications for supersymmetric flavor models", Nucl. Phys. **B 540** (1999) 37, and references therein

7. M. Beneke, G. Buchalla, I. Dunietz, "Mixing-induced CP asymmetries in inclusive B decays", Phys. Lett. **B 393** (1997) 132

8. A. Acuto, D. Cocolicchio, "CP asymmetries in neutral B-meson decays", Phys. Rev. **D 47** (1993) 3945

9. ALEPH Collaboration, "ALEPH: a detector for electron-positron annihilation at LEP", Nucl. Instr. Methods **A 294** (1990) 121

10. ALEPH Collaboration, "Performance of the ALEPH detector at LEP", Nucl. Instr. Methods **A 360** (1995) 481

11. T. Sjöstrand, M. Bengtsson, "The LUND Monte Carlo for jet fragmentation and e^+e^- physics", Comp. Phys. Comm. **43** (1987) 367

12. ALEPH Collaboration, "Heavy flavour production and decay with prompt leptons in the ALEPH detector", Z. Phys. **C 62** (1994) 179

13. ALEPH Collaboration, "A study of the decay width difference in the B_s^0–$\bar{B}_s^0$ system using $\phi\phi$ correlations", CERN-EP/2000-036, February 2000, accepted for publication by Phys. Lett. **B**

14. ALEPH Collaboration, "Update of electroweak parameters from Z decays", Z. Phys. **C 60** (1993) 71

15. ALEPH Collaboration, "A precise measurement of $\Gamma_{Z \to b\bar{b}}/\Gamma_{Z \to hadrons}$", Phys. Lett. **B 313** (1993) 535

16. ALEPH Collaboration, "Heavy quark tagging with leptons in the ALEPH detector", Nucl. Instr. Methods **A 346** (1994) 461

17. JADE Collaboration, "Experimental studies on multijet production in e^+e^- annihilation at PETRA energies", Z. Phys. **C 33** (1986) 23

18. ALEPH Collaboration, "Measurement of the B_s^0 lifetime", Phys. Lett. **B 322** (1994) 275

19. ALEPH Collaboration, "Study of the B_s^0–$\bar{B}_s^0$ oscillation frequency using $D_s^- \ell^+$ combinations in Z decays", Phys. Lett. **B 377** (1996) 205

20. ALEPH Collaboration, "Study of B_s^0 oscillations and lifetime using fully reconstructed D_s^- decays", Eur. Phys. J. **C 4** (1998) 367

21. C. Caso et al. (Particle Data Group), "Review of particle physics", Eur. Phys. J. **C 3** (1998) 1

22. The LEP Collaborations ALEPH, DELPHI, L3, OPAL, the LEP Electroweak Working Group and the SLD Heavy Flavour Groups, "A combination of preliminary electroweak measurements and constraints on the Standard Model", CERN-EP/2000-016, January 2000

23. ALEPH Collaboration, "Measurement of the b forward-backward asymmetry and mixing using high-$p_\perp$ leptons", Phys. Lett. **B 384** (1996) 414

24. I. Dunietz, "CP asymmetries in (semi-)inclusive B^0 decays", Eur. Phys. J. **C 7** (1999) 197

25. L. Lyons et al., "How to combine correlated estimates of a single physical quantity", Nucl. Instr. Methods **A 270** (1988) 110

26. OPAL Collaboration, "A study of B meson oscillations using hadronic Z^0 decays containing leptons", Z. Phys. **C 76** (1997) 401

27. OPAL Collaboration, "Measurement of the B^+ and B^0 lifetimes and search for CP(T) violation using reconstructed secondary vertices", Eur. Phys. J. **C 12** (2000) 609

28. CLEO Collaboration, "Two measurements of B^0–$\bar{B}^0$ mixing", Phys. Rev. Lett. **71** (1993) 1680; "Precise measurement of B^0–$\bar{B}^0$ mixing parameters at the $\Upsilon(4S)$", CLNS-00-1668, May 2000, submitted to Phys. Rev. Lett

29. CDF Collaboration, "Measurement of $b\bar{b}$ production correlations, B^0–$\bar{B}^0$ mixing, and a limit on ϵ_{B} in $p\bar{p}$ collisions at $\sqrt{s} = 1.8$ TeV", Phys. Rev. **D 55** (1997) 2546